AD-A154 787 A NUMERICAL STUDY OF TAYLOR-VORTEX FLOW(U) WISCONSIN UNIV-MADISON MATHEMATICS RESEARCH CENTER J C STRIKWERDA APR 85 MRC-TSR-2808 DAAG29-80-C-0041 1/1

UNCLASSIFIED F/G 20/4 NL

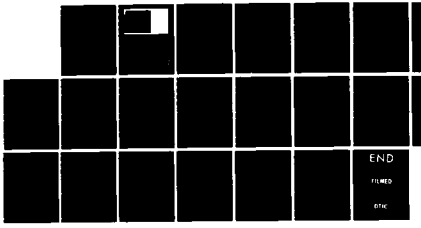

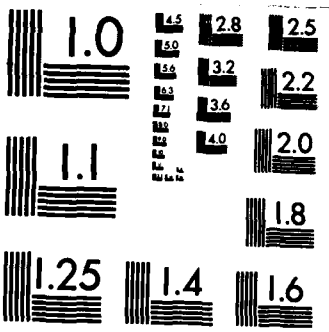

MRC Technical Summary Report #2808

A NUMERICAL STUDY OF TAYLOR-VORTEX FLOW

John C. Strikwerda

Mathematics Research Center
University of Wisconsin—Madison
610 Walnut Street
Madison, Wisconsin 53705

April 1985

(Received July 31, 1984

Approved for public release
Distribution unlimited

Sponsored by

U.S. Army Research Office
P. O. Box 12211
Research Triangle Park
North Carolina 27709

UNIVERSITY OF WISCONSIN-MADISON
MATHEMATICS RESEARCH CENTER

A NUMERICAL STUDY OF TAYLOR-VORTEX FLOW

John C.Strikwerda

Technical Summary Report #2808
April 1985

ABSTRACT

Results are presented of a numerical study of Taylor vortex flows. The computations were done with values of the Reynolds number and aspect ratio as used by T. B. Benjamin in his experiments. An extensive study was made of the two-cell and four-cell transitions and bifurcations. Good agreement was obtained with the experimental results. The flows were assumed to be axisymmetric so that the computation required only two spatial dimensions, although it required that all velocity components and the pressure be computed. A regularized central finite difference scheme was used to discretize the Navier-Stokes equations. The system of equations was solved by an iterative method similar to successive-over-relaxation.

AMS (MOS) Subject Classifications: 78D05

Key Words: Taylor vortices, Finite difference scheme,

Work Unit Number 3 (Numerical Analysis)

Sponsored by the United States Army under Contract No. DAAG29-80-C-0041.

SIGNIFICANCE AND EXPLANATION

Taylor-vortex flows have been studied extensively by fluid dynamicists because they provide relatively simple examples of bifurcations. In this report results are given of a study which used newly developed finite difference methods to solve the equations governing the flow. The study demonstrated the utility of the new methods and also gave new insights into certain aspects of Taylor-vortex flow.

The responsibility for the wording and views expressed in this descriptive summary lies with MRC, and not with the author of this report.

A NUMERICAL STUDY OF TAYLOR-VORTEX FLOW

John C. Strikwerda

1. *INTRODUCTION*

In this paper we present the results of a numerical study of Taylor-vortex motion in which finite difference methods were used to approximately solve the governing Navier-Stokes equations. Taylor vortices are generated in fluids confined between two concentric cylinders with the inner cylinder rotating at a fixed speed and with the outer cylinder held fixed. The numerical solutions of this study are compared with the experimental results of Benjamin (1978b). The numerical results agree quite closely with those of Benjamin and also reveal details which were not observed in the experiments.

Taylor-vortex motion is important in fluid dynamics because it provides a relatively simple example of bifurcation in steady fluid motion. A great deal of analysis has been done for the case of cylinders which are infinite in length and many experiments have been done for cylinders which is quite long compared with their radii. A good review of this work is in Di Prima (1981).

In contrast, Benjamin (1978b) conducted experiments with cylinders which were shorter than those of most previous experiments and he observed several new features. It is these observations of Benjamin which are the focus of the numerical investigations reported here. The features we shall concentrate on are first the nonuniqueness of the flow for certain values of the parameters, and secondly the nature of the bifurcations of the solutions. The study especially concentrated on the nature of the bifurcations between two-cell and four-cell flows.

Benjamin (1978a) also used the mathematical theory of bifurcations to explain the qualitative features of the bifurcations of the Taylor vortices. The numerical results of this paper are consistent with the explanations of the structure given by Benjamin.

Taylor-vortex flow provides a good basic test problem for numerical methods for the incompressible Navier-Stokes equations. The geometry is simple and yet the flows are non-

---

Sponsored by the United States Army under Contract No. DAAG29-80-C-0041.

trivial and this occurs at Reynolds numbers sufficiently low that good resolution can be obtained with a reasonable number of grid points. Furthermore there are experimental data with which to compare the numerical results.

Several other investigators have made numerical studies of Taylor-vortex flow. Several of these have been of the infinite cylinder case in which the flow is assumed to be periodic in the axial direction. The bifurcation phenomena are quite different than that studied here, see e.g. Meyer-Spache ıd Keller (1980). Calculations of the finite cylinder case have been made by Alziary de Roquefort and Grillaud (1978) at Reynolds numbers and aspect ratios greater than those considered here and they showed nonuniqueness of the solutions. The method they employed used the stream function and vorticity and they solved the time-dependent equations. Neitzel (1984) also used the stream function and vorticity with the time-dependent equations for cylinders with aspect ratios larger than 20. Related work has been done by Alonso and Macagno (1973) and Meyer (1966).

The previous numerical work closest to the present study in terms of the physical parameters is that of Cliffe (1983), Cliffe and Spence (1984), and Jones and Cliffe (1983). These use the finite element method on the steady-state equations. Cliffe (1983) and Cliffe and Spence (1984) study the bifurcation for flows with aspect ratio near 1.0, which we discuss in section 5. Jones and Cliffe (1983) study the four-cell and six-cell flows. Their results are similar to those of section 3 in which the two-cell and four-cell flows are studied. A finite difference method using a multigrid iterative method is also being used by Bolstad and Keller (1985) to study these problems.

The paper is organized as follows. In section 2 we present the differential equations which govern the flow and describe the numerical method which was used to solve the equations. Section 3 through 6 each deal with specific regimes of the parameters. Section 3 treats the nature of the two-cell and four-cell flows and the bifurcations between them. Section 4 treats the flow at low Reynolds numbers, including the case of zero Reynolds number. The bifurcation with aspect ratio 1.0 is described in section 5, and section 6 discusses the anomalous two-cell flow.

2. THE EQUATIONS

The experimental apparatus for generating Taylor-vortex motion consists of two coaxial cylinders with fluid filling the space between them. Let r_1 and r_2 be the radii of the inner and outer cylinders and let h be their height. The inner cylinder rotates with a constant angular velocity Ω. In Benjamin's experiments (Benjamin (1978b)) and in the calculations reported here the outer cylinder and the two end surfaces were fixed. The two basic parmeters governing the flow are the aspect ratio, Γ, and Reynolds number, R, given by

$$\Gamma = h/(r_2 - r_1)$$

$$Re = \Omega\, r_1(r_2 - r_1)/\nu$$

where ν is the kinematic viscosity. The motion generated by the rotation of the inner cylinder is primarily azimuthal, however, there is a secondary flow which is vortical in nature. The flow is axially symmetric.

The system of equations which describe axisymmetric flow between two cylinders is

$$\begin{aligned}
&- R^{-1}(\nabla^2 u - r^{-2}u) + r^{-1}(ru^2)_r + (wu)_z - r^{-1}v^2 + p_r = 0 \\
&- R^{-1}\nabla^2 w + r^{-1}(ruw)_r + (w^2)_z + p_z = 0 \qquad (2.1) \\
&- R^{-1}(\nabla^2 v - r^{-2}v) + r^{-1}(ruv)_r + (wv)_z + r^{-1}uv = 0 \\
&r^{-1}(ru)_r + w_z = 0 ,
\end{aligned}$$

where the subscripts denote differentiation and the scalar Laplacian is defined by

$$\nabla^2 q = r^{-1}(rq_r)_r + q_{zz} .$$

The domain on which the equations hold is

$$\eta \le r \le \eta + 1$$

$$0 \le z \le \Gamma .$$

The lengths have been non-dimensionalized by taking the distance between the cylinders as the reference length.

For Benjamin's experimental apparatus η was 1.597 and that was the value used in these computations. The other two parameters, R and Γ, were varied to produce the different flows.

The velocities were nondimensionalized using the velocity on the inner cylinder as the reference velocity. The boundary conditions then are

$u = w = 0$ on the boundaries

$v = 1$ on $r = \eta$

$v = 0$ on the other boundaries.

The finite difference scheme used to discretize the equations was basically the regularized central difference scheme presented in Strikwerda (1984a). The equations were discretized in the conservation form as written in the equations (2.1). The grid was uniform in both the r and z directions. Numerical values of the velocity and pressure were computed for each grid point.

For completeness, the finite difference scheme will be illustrated by giving the difference equations for the first and last equations of (2.1). They are

$$
\begin{aligned}
&- R^{-1}\Big(\frac{1}{r_i}\left(r_{i+\frac{1}{2}}(u_{i+1j} - u_{ij}) - r_{i-\frac{1}{2}}(u_{ij} - u_{i-1j})\right)/\Delta r^2 \\
&\quad + (u_{ij+1} - 2u_{ij} + u_{ij-1})/\Delta z^2 - u_{ij}/r_i^2 \\
&\quad + r_i^{-1}(r_{i+1}u_{i+1j}^2 - r_{i-1}^2 u_{i-1j})/2\Delta r \qquad (2.2) \\
&\quad + (w_{ij+1}u_{ij+1} - w_{ij-1}u_{ij-1})/2\Delta z \\
&\quad - r_i^{-2} v_{ij}^2 \\
&\quad + \left(p_{i+1j} - p_{i-1j} - (p_{i+2j} - 3p_{i+1j} + 3p_{ij} - p_{i-1j})/3\right)/2\Delta r \\
&\quad = 0 .
\end{aligned}
$$

and

$$r_i^{-1}\left(r_{i+1}u_{i+1j} - r_{i-1}u_{i-1j} - (u_{i+1j} - 3u_{ij} + 3u_{i-1j} - u_{i-2j})/3\right)/2\Delta r$$

$$+ \left(w_{ij+1} - w_{ij-1} - (w_{ij+1} - 3w_{ij} + 3w_{ij-1} - w_{ij-2})/3\right)/2\Delta z \qquad (2.3)$$

$$= \delta_h \, .$$

The use of the regularizing third divided differences on the p_r and p_z terms and on the divergence of the velocity are explained in Strikwerda (1984a), as is the need for the constant δ_h in (2.3). In all of the computed solutions δ_h was 10^{-4} or smaller.

The iterative method used to solve the finite difference equations was a variant of the method described in Strikwerda (1984b). The iterative method consisted of a point S.O.R. update of the velocities using the natural ordering followed by an update of pressure, and then another point S.O.R. update of the velocity using the reverse ordering. This symmetric S.O.R. version seemed more robust than the version with only one S.O.R. update.

The iterative procedure was stopped when the residuals of the difference equations were less than a specified tolerance which was usually 10^{-4}, but near bifurcation points the tolerance was sometimes 10^{-5} or 10^{-6}.

3. THE TWO-CELL AND FOUR-CELL FLOWS

A fairly extensive study was made of the bifurcations and transitions between two-cell and four-cell flows. The bifurcation and transition points are displayed in Figure 3.1. For values of R and Γ to the right of the curve ACB the solutions are not unique. Solutions can have either two or four vortex cells. To the left of curve ACB the solutions are unique. Above the curve DCA the solutions have four cells and below DCB they have two cells.

Several quantities obtained from the computed solution were tabulated to aid in the analysis of the solutions. The most useful quantity was found to be the average value of the radial component of the velocity at the midplane, i.e. at $z = \Gamma/2$. Since this quantity, which we denote by $\bar{u}_{1/2}$ is positive for two-cell flows and negative for four-cell flows it provides a convenient indicator of the transition between the two types of flows.

The graphs of $\bar{u}_{1/2}$ as a function of R for several values of Γ are displayed in Figure 3.2. Figure 3.1 and Figure 3.2 together illustrate the nature of the transitions and bifurcations between the two-cell and four-cell flows. For example, for Γ equal to 3.80, Figure 3.2 has two curves. For values of R greater than 82 there is a curve for which $\bar{u}_{1/2}$ is positive, corresponding to a two-cell flow, and a curve for which $\bar{u}_{1/2}$ is negative, corresponding to a four-cell flow. The four-cell flow exists for all values of R displayed in Figure 3.2, whereas the two-cell flow exists only for R greater than approximately 81.5. Figure 3.3 displays the radial and axial velocity components of the two-cell and four-cell flows for R equal to 85 and Γ equal to 3.8.

For Γ equal to 3.70, the situation is similar except it is the upper curve in Figure 3.2 which is defined for all values of R displayed, and the lower curve which exists only for larger R. An additional feature is that the upper curve represents a two-cell flow for R larger than about 78.0 and a four-cell flow for smaller values of R.

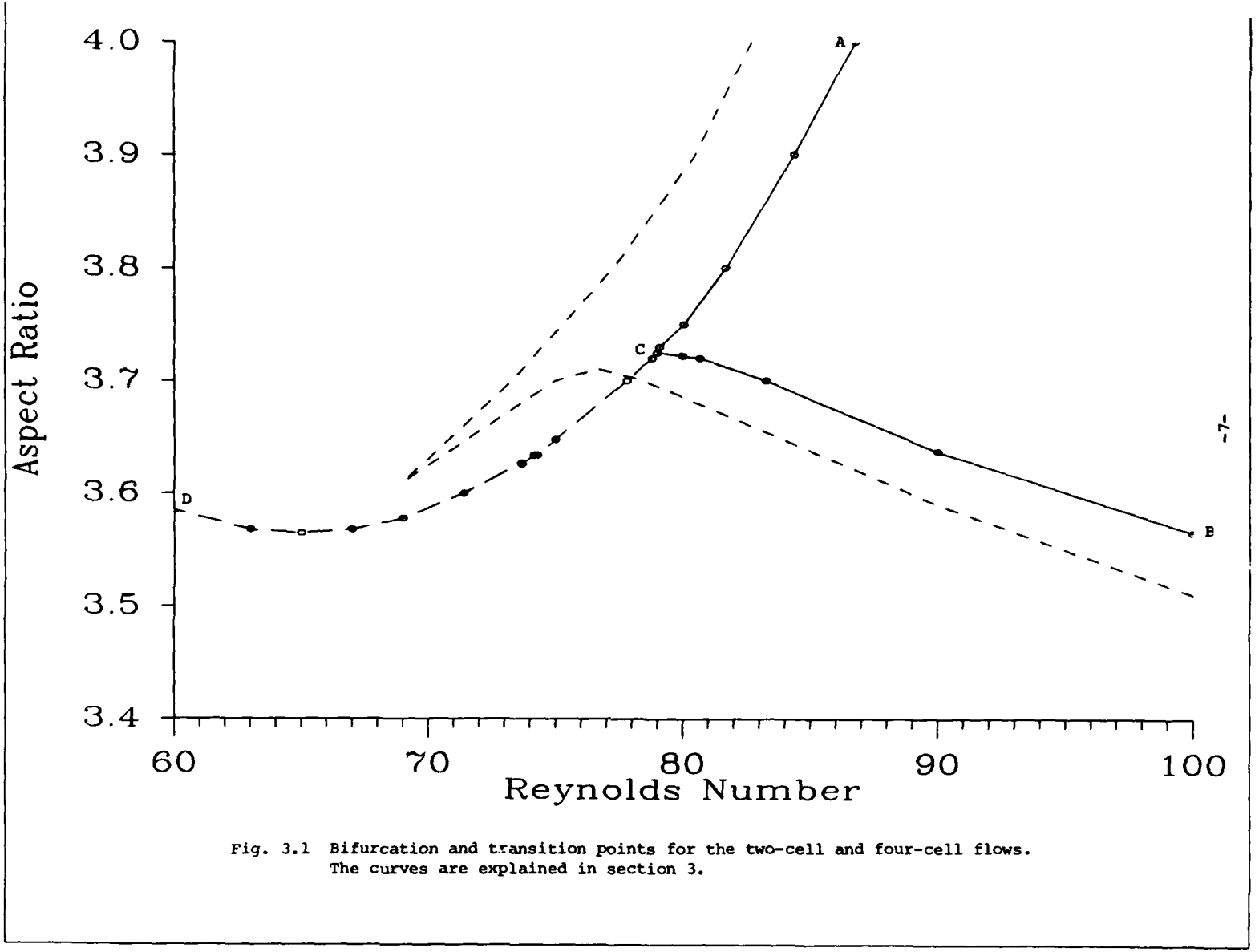

Fig. 3.1 Bifurcation and transition points for the two-cell and four-cell flows. The curves are explained in section 3.

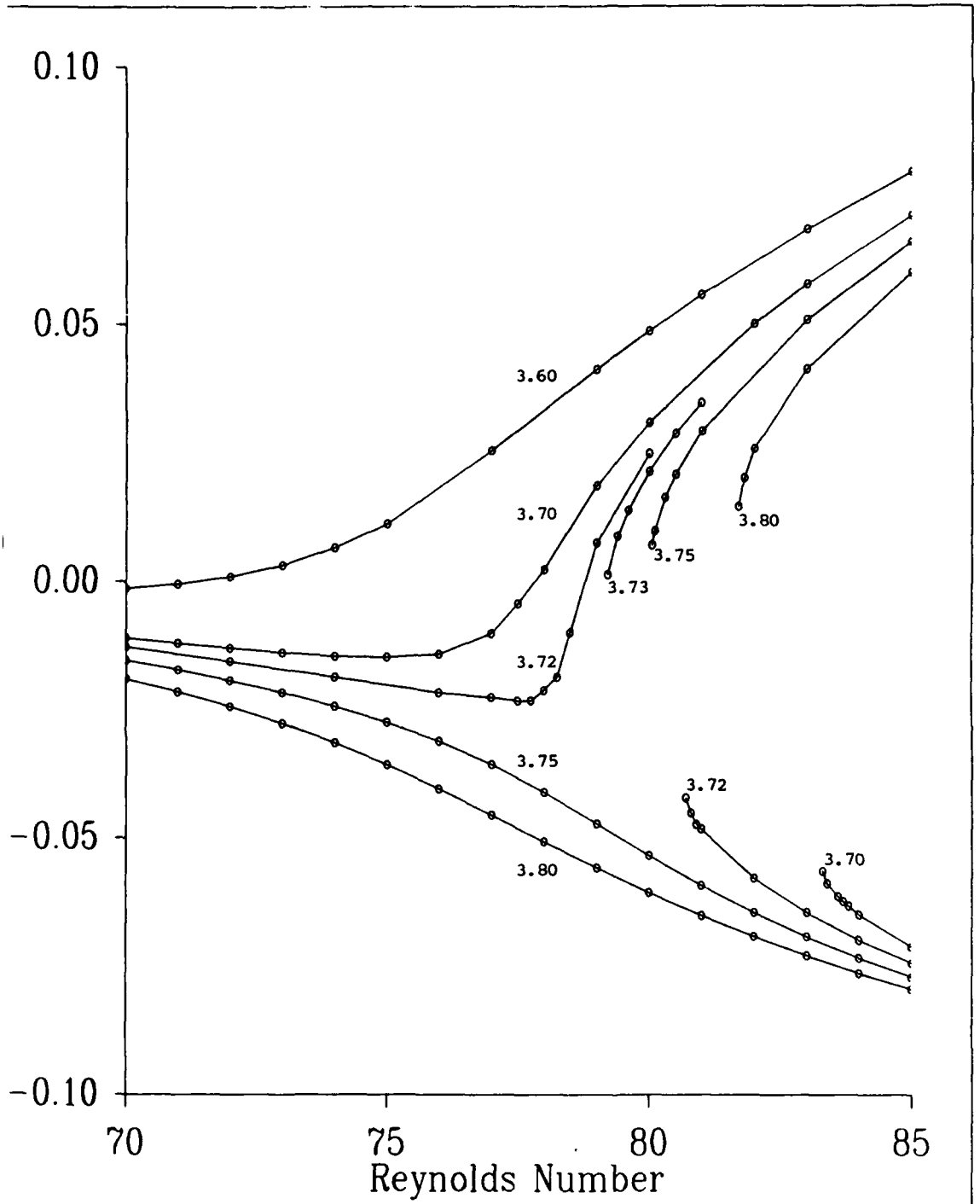

Fig. 3.2 Plot of the average value of the radial velocity at the midplane as a function of Reynolds' number for several values of the aspect ratio.

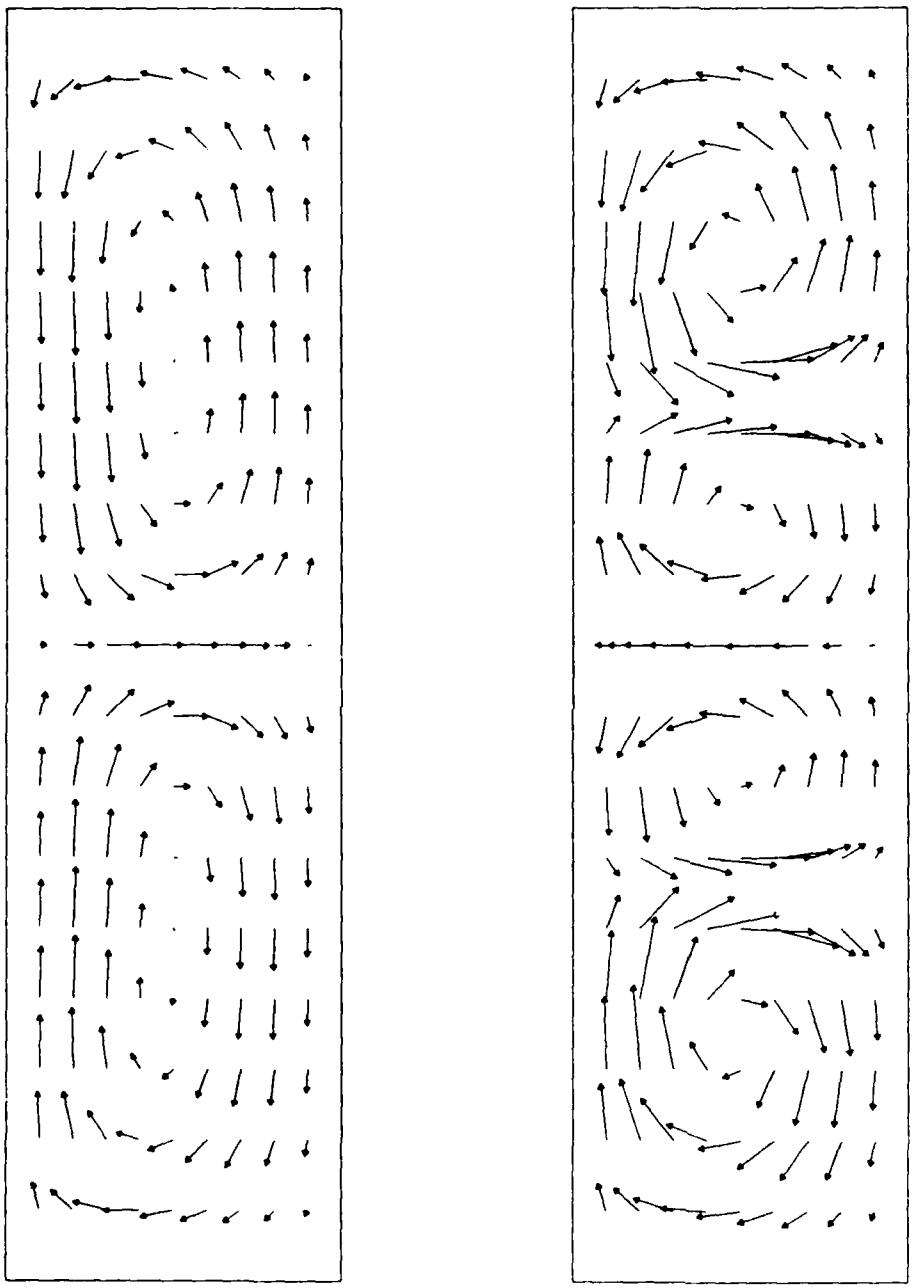

Fig. 3.3 Plot of the radial and axial velocity components for the two-cell and four-cell flows for R = 85 and Γ = 3.80 For each flow the rotating inner cylinder is on the left and the stationary outer cylinder is on the right.

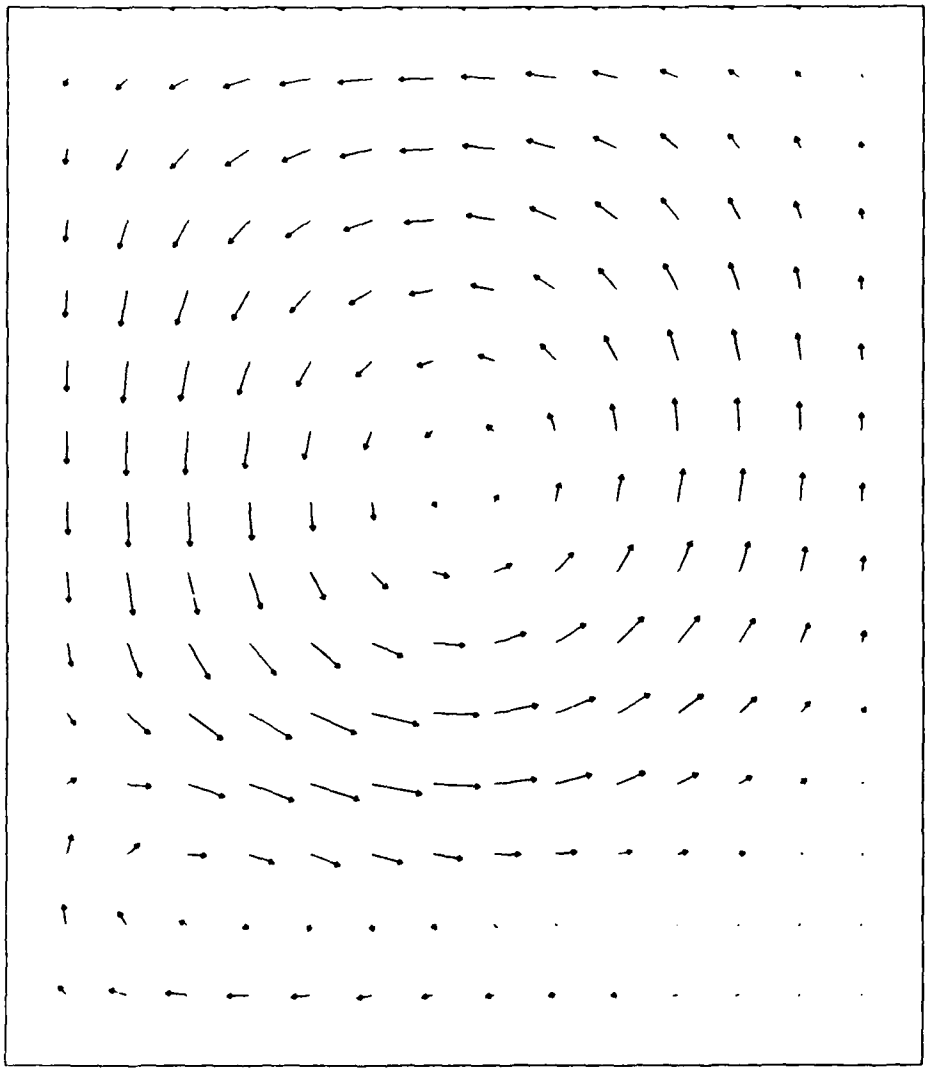

Fig. 6.1 Plot of the radial and axial velocity componenets for $R = 225$ and $\Gamma = 2.30$. The plot shows only the lower half of the solution which is symmetric about the midplane.

6. THE ANOMALOUS TWO-CELL FLOWS

In addition to the anomalous one-cell flow described in section 5, the anomalous two-cell flow seen by Benjamin was also investigated. The anomalous two-cell flow was computed by starting with an initial iterate that had two vortices rotating opposite to the normal two-cell flow. The iterative process required some adjustment to obtain the desired solution from this initial iterate. Converged solutions are displayed in Figures 6.1 and 6.2 for a Reynolds' number of 225 and aspect ratio of 2.30. Notice the presence of the small normal cells in the corners. As in the anomalous one-cell flow discussed in section 5, one sees that the flow is a normal flow with the two end cells being confined to small regions in the corners by the inner cylinders.

The similarity between the lower half of Figure 6.1 and the anomalous one-cell flow of Figure 5.3 suggests that it might be possible to continuously transform the anomalous two-cell flow of Figure 6.1 to a normal four-cell flow at lower values of the Reynolds' number. However, all attempts at this failed. For all values of the aspect ratio, reduction of the Reynolds number eventually led to a bifurcation to a normal two-cell flow. Also for fixed values of the Reynolds number, either increasing or decreasing the aspect ratio ultimately led to a normal two-cell solution. For example, for a Reynolds number of 225, the anomalous two-cell flow was computed only for values of the aspect ratio between about 2.0 and 2.322.

It was also considered possible that the bifurcation could be prevented if the solutions were forced to be symmetric about the mid-plane of the flows (i.e. at z equal to $\Gamma/2$). However, this had no effect on the bifurcations. Because this was computationally more efficient most of anomalous two-cell flows were computed using only half of the domain with symmetry boundary conditions on the midplane.

In addition to the two asymmetric flows discussed above, there is a symmetric solution to the equations (2.1) with $\Gamma = 1.0$ and R greater than $R_c(1.0)$. However, this flow is dynamically unstable and is not observed experimentally. It is also unstable for the iterative algorithm by which the numerical solutions were obtained. However, this unstable symmetric solution can be obtained numerically by computing on only the region $0 \leq z \leq .5$ and imposing symmetry boundary conditions at $z = 0.5$.

The values of $\bar{u}$ computed for this half-region solution are also displayed in Fig. (5.4). For R less than 149 there is a deviation in the values of $\bar{u}$ between the full-region solutions and the half-region solutions of about one percent. This is because the numerical symmetry conditions for the half-region solution are not exactly satisfied by the full-region solution. The values of $\bar{u}$ for the symmetric solutions display no evidence of the bifurcation point, as is to be expected.

To further demonstrate that the symmetric flows are unstable for R greater than $R_c(1.0)$ a full-region solution was obtained by "doubling" the half-region solution for R equal to 154. The symmetric flow so obtained is not quite a solution of the difference equations for the full-region because of the symmetry boundary approximations applied to the half-region solution. The iterative solution algorithm applied to this flow ultimately converged to an asymmetric flow. All of the flows with aspect ratio 1.0 were computed on a grid with 33 points in each direction, except for the half-region solution which was computed on a 17 by 33 grid.

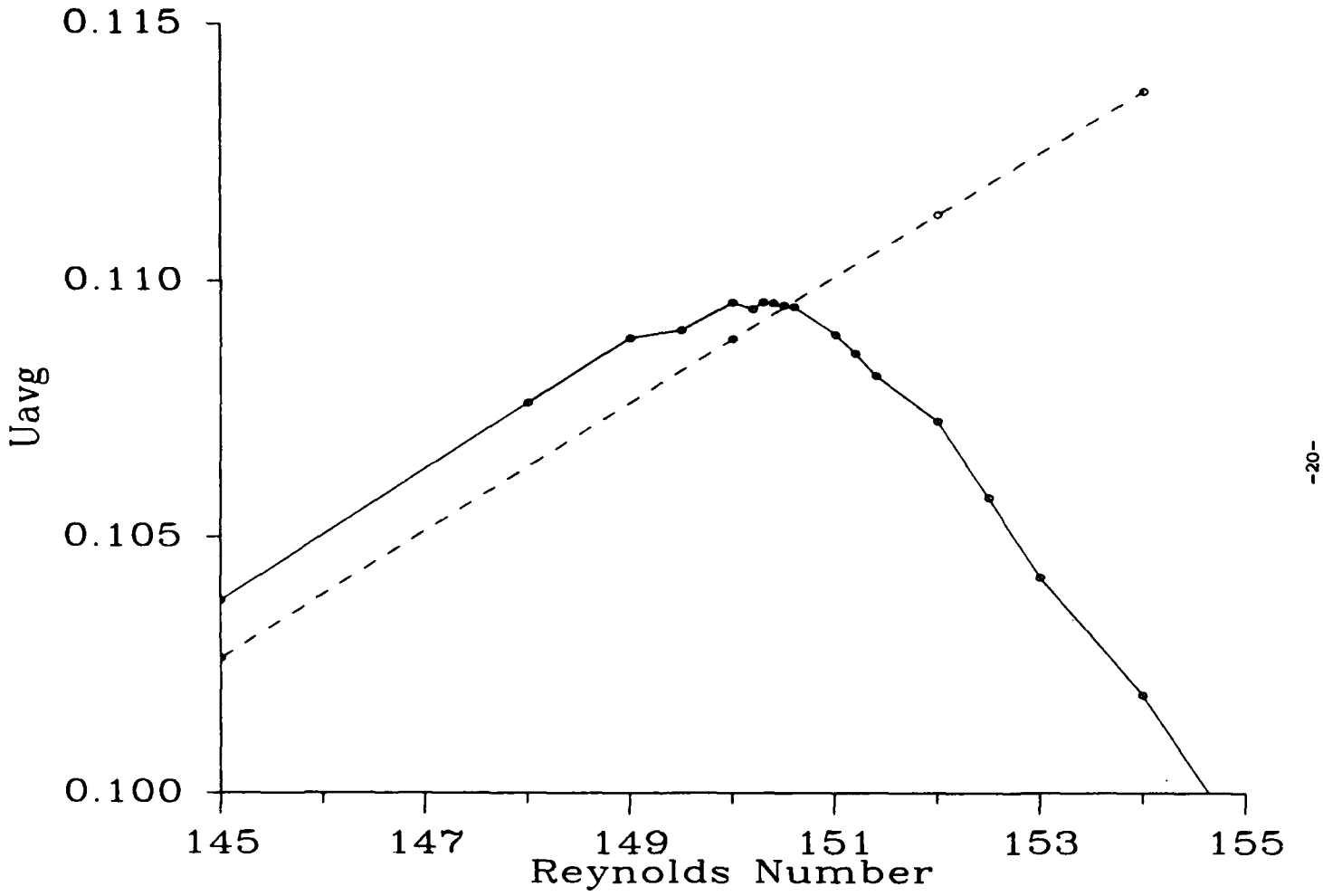

Fig. 5.4 Plot of the average value of the radial velocity at the midplane as a function of Reynolds' number for $\Gamma = 1$. The dashed line is for the symmetric solution.

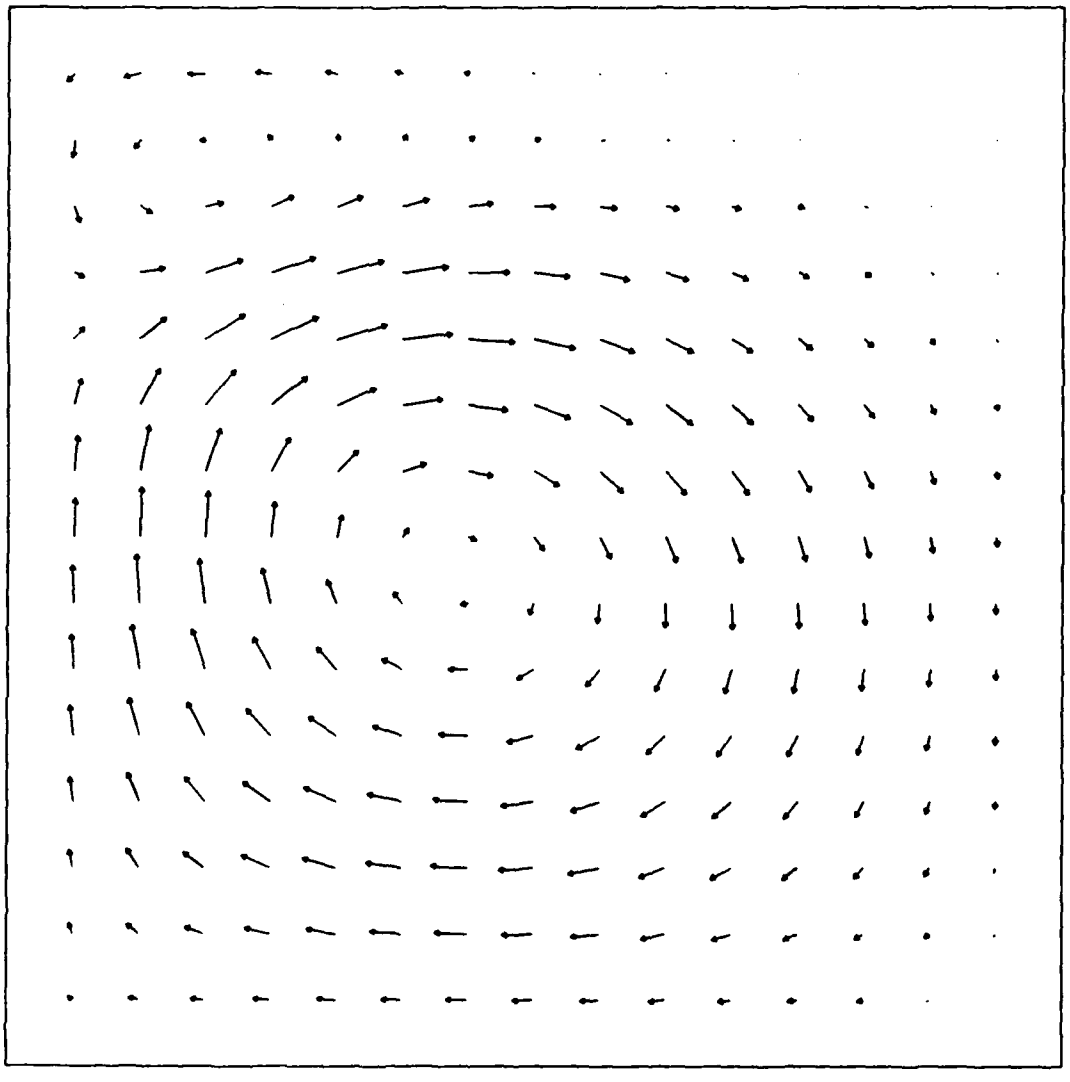

Fig. 5.3 Plot of the radial and axial velocity components for $R = 200$ and $\Gamma = 1$.

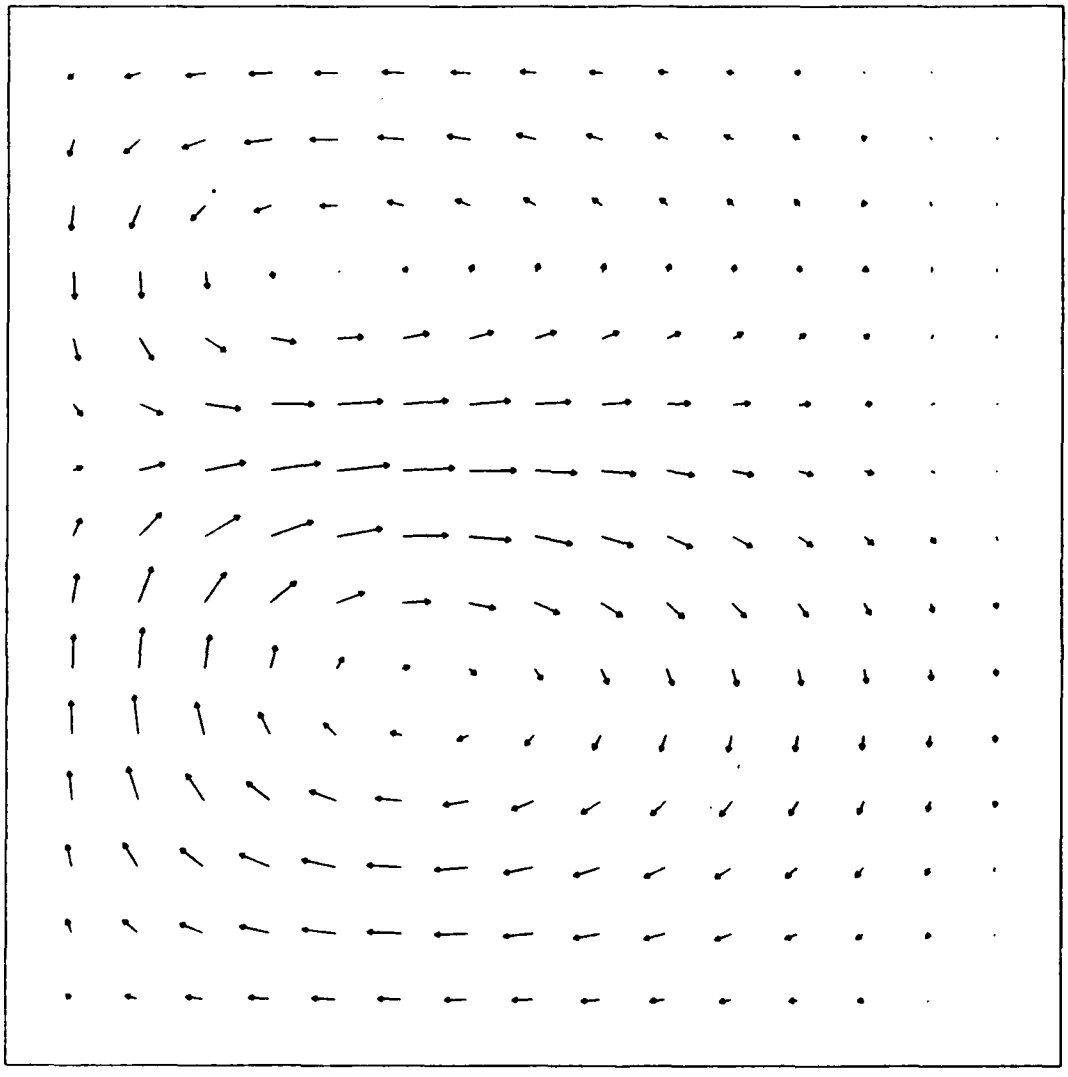

Fig. 5.2 Plot of the radial and axial velocity components for $R = 155$ and $\Gamma = 1$.

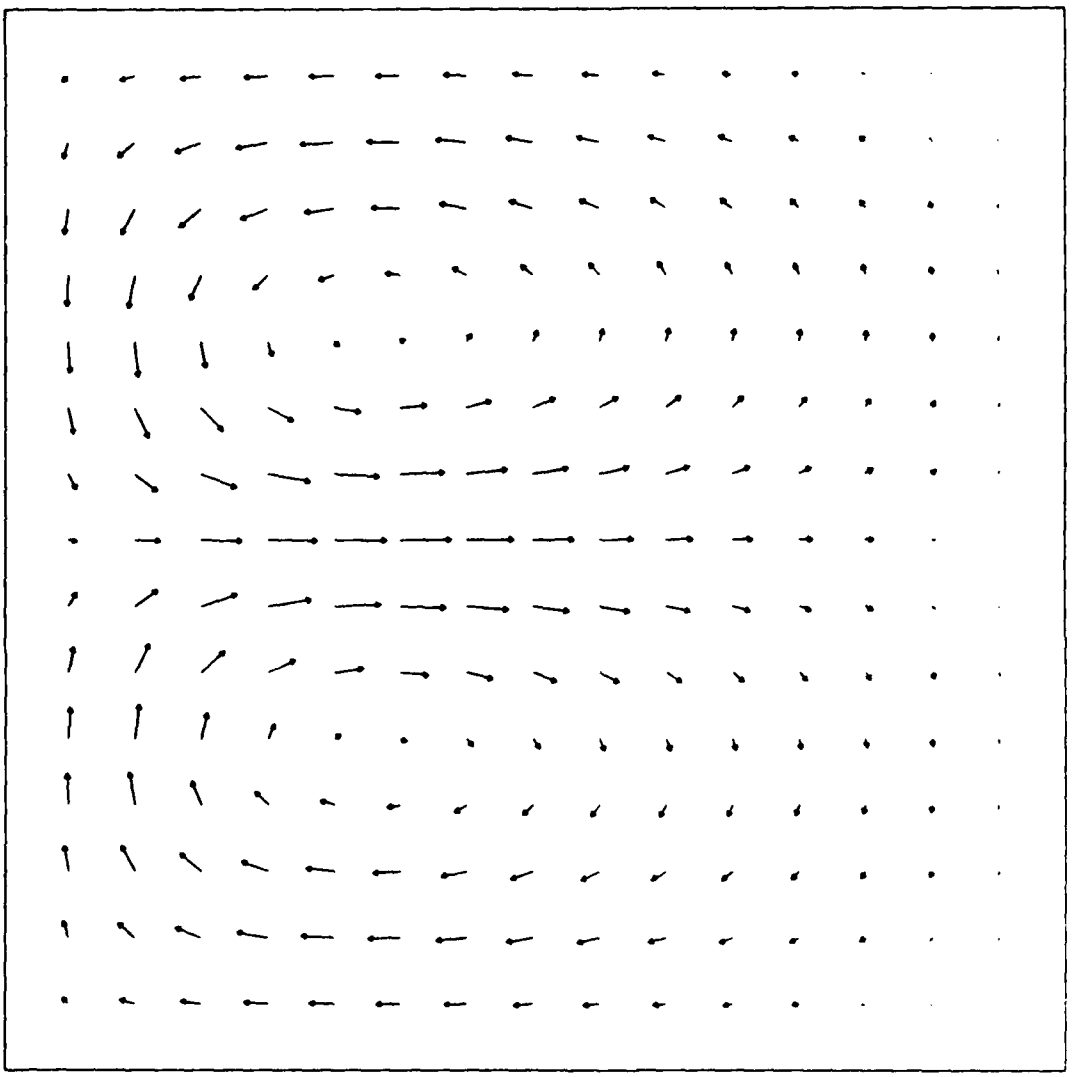

Fig. 5.1 Plot of the radial and axial velocity components for $R = 145$ and $\Gamma = 1$.

5. BIFURCATION WITH ASPECT RATIO OF 1.0

In this section we discuss the results of computations done with the aspect ratio fixed at 1.0. Benjamin (1978b) reported a symmetry breaking bifurcation for this aspect ratio, with the resulting flow becoming an anomalous one-cell flow. The numerical calculations confirm this observation and give added insight into the flow behavior. Cliffe (1983) has done an extensive study of flows with aspect ratio near 1.0. The results given here agree well with those of Cliffe.

When the aspect ratio is 1.0 the primary flow is symmetric about the midplane with two counter-rotating vortex cells (see Fig. 5.1). However, for Reynolds numbers larger than a critical value, $R_c(1.0)$, the symmetric flow is unstable. For Reynolds numbers slightly larger than $R_c(1.0)$ there are two stable flows consisting of two counter-rotating vortex cells but with one cell larger than the other, (see Fig. 5.2). The larger cell can be either the top or the bottom cell, indeed the two flows are reflections of each other about the line $\Gamma = 0.5$.

As the Reynolds number is further increased the larger of the two cells increases in size, filling most of the flow region. Correspondingly, the smaller cell decreases in size finally being confined to a small region near the inner cylinder and the top or bottom surface (see Fig. 5.3). Benjamin characterized these flows as anomalous one-cell flows, the anomaly being that the dominant cell is flowing outward at either the top or bottom surface. There is no evidence of his having noticed the smaller cell. Thus the anomalous flow is a normally circulating flow with one end cell being significantly reduced in size.

To illustrate the nature of this bifurcation we have plotted the average value of the radial component of velocity $\bar{u}$ along the line $z = .5$ as a function of Reynolds number in Fig. 5.4. For R less than 149 the flows are symmetric and $\bar{u}$ varies almost linearly with R. For R greater than about 149.0 the flows are asymmetric and $\bar{u}$ deviates from the linear relation which held for R below 149.0 The asymmetric flows occur with the larger cell either at the top or at the bottom.

This implies that for sufficiently small values of the Reynolds number the primary flow has only two cells. Since for larger values of the Reynolds number the primary flow can have any even number of vortices, this number depending on the aspect ratio, there must be an addition of vortex cell pairs as the Reynolds number is increased.

We examined in more detail the flow with aspect ratio 4.0, and beginning with the flow at Reynolds number of zero, increased the Reynolds number to locate the value at which a new vortex pair appeared. The transition from two cells to four cells occurred for a Reynolds number of about 41.0. This was a smooth transition with the new vortex pair occurring in the Couette flow region between the stronger pair. This transition is well away from, and should not be confused with, the bifurcations associated with the two-cell and four-cell flows which are discussed in section 3.

For the Reynolds number equal to zero the Couette flow between the vortex pair was compared with the Couette flow between cylinders with infinite aspect ratio. It was found that for the aspect ratio of 6.0 the azimuthal velocity and the pressure at the midplane, i.e. $z = .5\Gamma$, of the computed solution agreed to within one percent with the values of the infinite aspect ratio Coette flow.

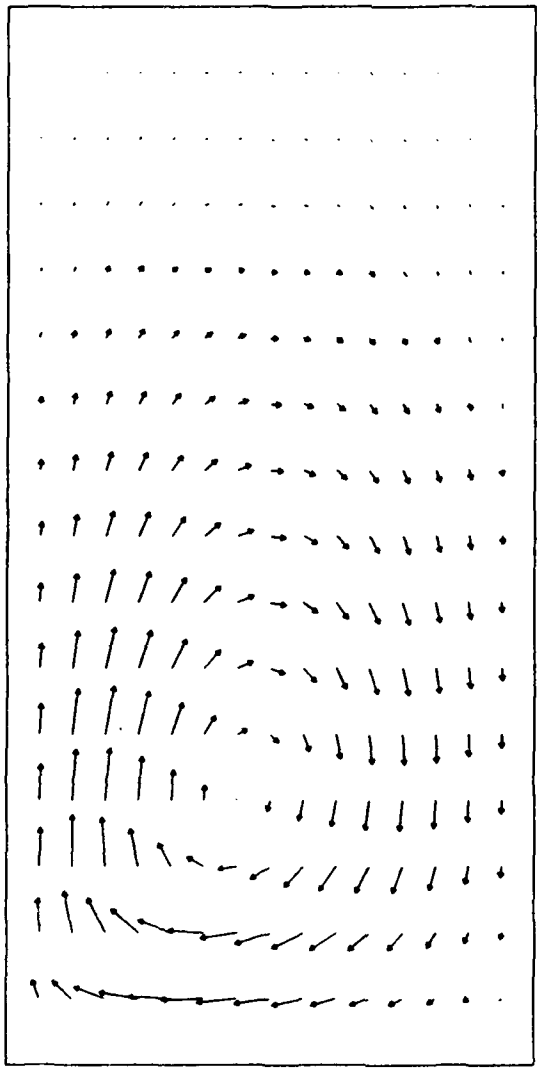

Fig. 4.1 Plot of the radial and axial velocity components for $R = 0$ and $\Gamma = 4$.

4. THE FLOW AT LOW REYNOLDS NUMBER

This section is concerned with the determination of the flow for small values of the Reynolds number, including the case when the Reynolds number is equal to zero. As the Reynolds number tends to zero in Equation (2.1), the axial and radial velocity components tend to zero. By considering the derivatives of these velocity components with respect to the Reynolds number we obtain the system

$$\begin{aligned} -(\nabla^2 u' - u'/r^2) + p'_r &= v^2/r \\ -\nabla^2 w' + p'_z &= 0 \\ -(\nabla^2 v - v/r^2) &= 0 \\ \tfrac{1}{2}(ru')_r + w'_z &= 0 \end{aligned} \qquad (4.1)$$

where $u' = \frac{\partial u}{\partial R}|_{R=0}$, $w' = \frac{\partial w}{\partial R}|_{R=0}$ and $p' = \frac{\partial (Rp)}{\partial R}|_{R=0}$.

The boundary conditions for (4.1) are that u' and w' are zero on the whole boundary and v has the same boundary conditions as in section 2. Notice that in (4.1) v is not dependent on u', w', or p'.

The system (4.1) was solved for several values of the aspect ratio. The solutions were all qualitatively the same, consisting of two counter-rotating cells, one at the top and one at the bottom. Figure 4.1 displays the axial and radial velocity for a solution obtained by using the symmetry conditons at the mid-plane of the cylinders.

Since Laplace's equation and the Stokes' equations have unique solutions, the system (4.1) also has a unique solution. That the unique solution is essentially that which was computed is attested to by the fact that the two-cell solutions were computed from a number of initial approximations. In particular, initial approximations with four cells gave rise to the two-cell structure as displayed in Figure 4.1. Thus we conclude that for the Reynolds number equal to zero the flow has two cells for all values of the aspect ratio.

Reynolds No.	Aspect Ratio
Bifurcation points	
100.	3.565
90.	3.637
83.28	3.70
80.67	3.72
80.	3.722
79.	3.725
86.77	4.00
84.38	3.90
81.69	3.80
80.04	3.75
79.1	3.73
Transition points	
78.8	3.72
77.82	3.70
75.00	3.648
74.275	3.634
74.14	3.634
73.68	3.626
73.66	3.627
71.4	3.60
69.0	3.578
67.0	3.568
65.0	3.565
63.0	3.568
60.0	3.585
58.3	3.60

Table 3.1

quantity $(u^2 + w^2)^{1/2}$. For each of the values listed in Table 3.1 the estimates of the bifurcation point were in agreement to the number of digits shown for all three indicators.

Figure 3.1 also displays approximately the bifurcation curve determined by Benjamin (1978b) for the two-cell and four-cell bifurcation. The bifurcation curve corresponding to CA differs in location by about five percent in the Reynold number and the curves corresponding to CB differ by about three percent in the aspect ratio. These differences are not regarded as significant.

Of greater significance is the nature of the cusp at the point C. Benjamin (1978b) found it to be a long narrow cusp. He did not determine the location of the transition line corresponding to DC. In the numerical calculations the cusp was not as narrow, with the transition line in the location where the narrow cusp was expected, based on Benjamin's results. Great care was taken to insure that the flows near the transition line were indeed unique. Many solutions were computed near the transition line and no evidence of bifurcation was found.

This disagreement between the experimental and numerical studies can be explained several ways. First, however, it should be emphasized that the flows in the region of the cusp are not easy to obtain, either experimentally (Benjamin, (1978b)) or numerically. Experimentally, the flows take a long time to settle to a steady state. Numerically, the nearly singular Jacobian of the nonlinear system in this region curves causes the iterative method to converge slowly. The disagreement on the nature of the cusp could result from the experimental observations being made before the fluid had reached a steady state, that is, before the very weak vortex motion at the midsection had stabilized. It is also possible that the numerical approximation was not sufficiently accurate to faithfully represent the narrow cusp.

A comparison of Figure 3.2 with Figure 3.1 shows that the curve DC of Figure 3.1 represents a smooth transition between two-cell and four-cell flows, while CA marks a bifurcation for two-cell flows and CB marks a bifurcation for four-cell flows.

Table 3.1 lists several bifurcation points for the curves CA and CB of Figure 3.1. The values of the bifurcation points were computed by fitting R or Γ as a quadratic function of $\bar{u}_{1/2}$ using three solutions near the bifurcation point. For example, for the ninth entry where Γ is 3.80 a series of solutions was computed with R equal to 85, 83, 82, 81.8, and 81.7. Beginning with the first three solutions, and then with each successive group of three, R was determined as a quadratic function of $\bar{u}_{1/2}$. The bifurcation point was estimated as that value of R where the derivative with respect to $\bar{u}_{1/2}$ of the quadratic approximation of R was zero. Successive solutions nearer the bifurcation point were computed until the estimate did not vary in as many decimal places as are shown in the table. As the bifurcation point was approached the number of iterations required to compute a solution increased dramatically. For example, starting with the solution for R equal to 83, the solution with R equal to 82 took 392 iterations, while starting with R of 81.8 and computing the case with R of 81.7 took 865 iterations.

The grids had 21 points in the radial direction and 73 in the axial direction, and one iteration took approximately 2 cpu seconds. The fact that so many solutions could be computed in reasonable amounts of time speaks for the efficiency of the iterative method.

The estimate of the bifurcation points obtained from three successive solutions was also used as a measure of the accuracy of the solution. If the iterative procedure was stopped before the finite difference equations were sufficiently satisfied, the estimates of the bifurcation points were erratic. In general, the tolerances on the residuals had to be reduced as the bifurcation points were approached in order to obtain a satisfactory solution and good estimates of the bifurcation points.

Other quantities were also used to estimate the bifurcation points. The most useful were the difference in the maximum and minimum of the pressure and the maximum of the

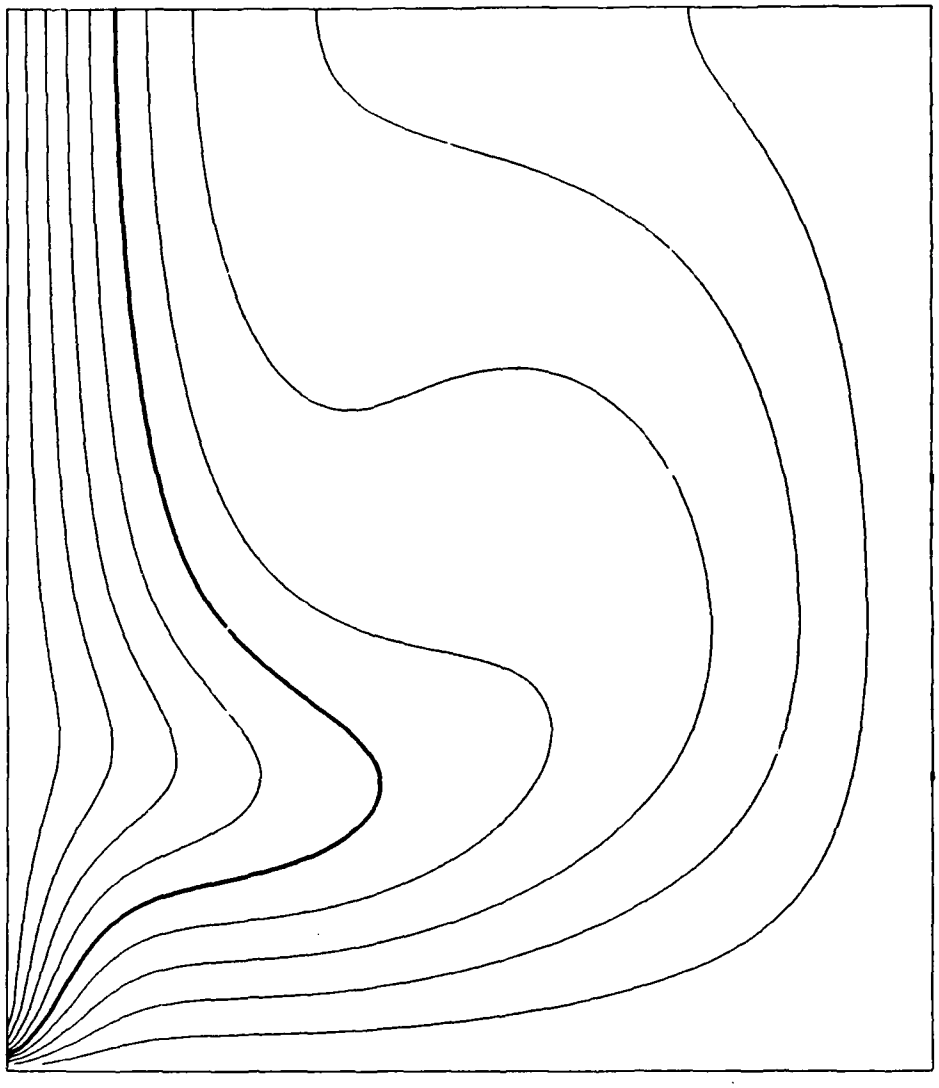

Fig. 6.2 Contour plot of the azimuthal velocity component for $R = 225$ and $\Gamma = 2.30$.

7. CONCLUSION

The numerical study of Taylor vortex motion discussed in this report serve to increase our understanding of the bifurcation phenomena of fluid dynamics. The investigation has also demonstrated the usefulness of the finite difference methods which were used. Calculations using the basic method on other problems are in progress and will be reported in due course.

Acknowledgement

I wish to thank Mr. T. Grandine and Mr. K. Knapp for their assistance with the coding and graphics.

REFERENCES

[1] Alonso, C. V. and E. O. Macagno, (1973) Numerical integration of the time-dependent equations of motion for Taylor vortex flow, Comput. Fluids, 1, 301-316.

[2] Alziary de Roquefort, T. and G. Grillaud, 1978, Computation of Taylor Vortex Flow by a Transient Implicit Method, Comput. Fluids, 6, 259-269.

[3] Benjamin, T. B., 1978a, Bifurcation phenomena in steady flows of a viscous fluid, I. Theory. Proc. R. Soc. Lond. A. 359, 1-26.

[4] Benjamin, T. B., 1978b, Bifurcation phenomena in steady flows of a viscous fluid, II. Experiments. Proc. R. Soc. Lond. A. 359, 27-43.

[5] Benjamin, T. B. and T. Mullin, 1981, Anomalous modes in the Taylor experiment. Proc. R. Soc. Lond. A. 377, 221-249.

[6] Bolstad, J. H. and H. B. Keller, (1985) Taylor vortex flows by multigrid methods, to appear.

[7] Cliffe, K. A. 1983, Numerical calculations of two-cell and four-cell Taylor flows. J. Fluid Mech. 135, 219-233.

[8] Cliffe, K. A. and A. Spence, 1984, The calculation of high order singularities in the finite Taylor problem. Numerical Methods in Bifurcation Problems, ISNM Birkhauser Basel.

[9] DiPrima, R., 1981, Transition in Flow between Rotating Concentric Cylinders. Transition and Turbulence ed. R. E. Meyer. Academic Press.

[10] Jones, I. P. and K. A. Cliffe, 1983, Numerical Solutions for Flows due to Rotating Cylinders and Disks, presented at Fifth Workshop on Gases under Strong Rotation, U. of Virginia, Charlottesville.

[11] Meyer, K. A. (1966), A two-dimensional time-dependent numerical study of rotational couette flow, Los Alamos Scientific Laboratory Report LA-3497.

[12] Meyer-Spache, R. and H. B. Keller, 1980, Computations of the Axisymetric Flow between Rotating Cylinders, J. Comp. Phys. 35, 100-109.

[13] Neitzel, G. P. 1984, Numerical Computation of Time-Dependent Taylor-Vortex Flows in Finite Length Geometries. J. Fluid Mech. 141, 51-66.

[14] Strikwerda, J. C. 1984a, Finite difference methods for the Stokes and Navier-Stokes equations. SIAM J. Sci. Stat. Comput. 5, 56-68.

[15] Strikwerda, J. C.1984b, An iterative method for solving finite difference approximations to the Stokes equations. SIAM J. Numer. Anal. 21, 447-458.

JS:jp

SECURITY CLASSIFICATION OF THIS PAGE (When Data Entered)

REPORT DOCUMENTATION PAGE		READ INSTRUCTIONS BEFORE COMPLETING FORM
1. REPORT NUMBER #2808	2. GOVT ACCESSION NO. A154787	3. RECIPIENT'S CATALOG NUMBER
4. TITLE (and Subtitle) A NUMERICAL STUDY OF TAYLOR VORTEX FLOW		5. TYPE OF REPORT & PERIOD COVERED Summary Report - no specific reporting period
		6. PERFORMING ORG. REPORT NUMBER
7. AUTHOR(s) John C. Strikwerda		8. CONTRACT OR GRANT NUMBER(s) DAAG29-80-C-0041
9. PERFORMING ORGANIZATION NAME AND ADDRESS Mathematics Research Center, University of Wisconsin 610 Walnut Street Madison, Wisconsin 53706		10. PROGRAM ELEMENT, PROJECT, TASK AREA & WORK UNIT NUMBERS Work Unit Number 3 - Numerical Analysis and Scientific Computing
11. CONTROLLING OFFICE NAME AND ADDRESS U. S. Army Research Office P.O. Box 12211 Research Triangle Park, North Carolina 27709		12. REPORT DATE April 1985
		13. NUMBER OF PAGES 27
14. MONITORING AGENCY NAME & ADDRESS(if different from Controlling Office)		15. SECURITY CLASS. (of this report) UNCLASSIFIED
		15a. DECLASSIFICATION/DOWNGRADING SCHEDULE

16. DISTRIBUTION STATEMENT (of this Report)

Approved for public release; distribution unlimited.

17. DISTRIBUTION STATEMENT (of the abstract entered in Block 20, if different from Report)

18. SUPPLEMENTARY NOTES

19. KEY WORDS (Continue on reverse side if necessary and identify by block number)

Taylor vortices
Finite difference scheme

20. ABSTRACT (Continue on reverse side if necessary and identify by block number)

Results are presented of a numerical study of Taylor vortex flows. The computations were done with values of the Reynolds number and aspect ratio as used by T. B. Benjamin in his experiments. An extensive study was made of the two-cell and four-cell transitions and bifurcations. Good agreement was obtained with the experimental results. The flows were assumed to be axisymmetric so that the computation required only two spatial dimensions, although it required that all velocity components and the pressure be computed.

(over)

DD FORM 1 JAN 73 1473 EDITION OF 1 NOV 65 IS OBSOLETE

UNCLASSIFIED

SECURITY CLASSIFICATION OF THIS PAGE (When Data Entered)

20. A regularized central finite difference scheme was used to discretize the Navier-Stokes equations. The system of equations was solved by an iterative method similar to successive-over-relaxation.

END

FILMED

7-85

DTIC